640
doi:10.1017/S1431927613005199

Microsc. Microanal. 19 (Suppl 2), 2013


# Applications of MicroCT in Earth Sciences

Brian Bagley[1] and Jonathan Keller[2]

[1.] Department of Earth Sciences, University of Minnesota, Minneapolis, MN, USA.
[2.] Department of Ecology, Evolution, and Behavior, University of Minnesota, Saint Paul, MN, USA.

The current generation of microCT machines is capable of sub-micron defect recognition, making them useful for a host of Earth science research topics. The following are four in-progress case studies being conducted at the University of Minnesota (UMN) microCT facility (xraylab.esci.umn.edu).

Case study 1: Changes in permeability and pore-scale geometries from *in-situ* microCT
*In-situ* microCT experiments will document changes in permeability and pore-scale geometries of serpentinized olivine-rich samples. These experiments are designed to explore interactions of chemical and physical processes of feedback by fluid and mineral components as fluids flow through confined core samples. 3D reconstructions of pore and solid geometries (Fig. 1) of ongoing experiments will link chemical reactions, pore geometries, and resultant permeability fields.

Case study 2: Microfabric analysis of high and ultrahigh pressure eclogite and host migmatite
Using microCT, the Structure Tectonics and Metamorphic Petrology (STAMP) research group is developing new methods to build a large dataset to assess fabric variations on local and regional scales. MicroCT will characterize the 3D shape and distribution of minerals (Fig. 2). In the host gneisses, we will image biotite and amphibole then determine the bulk fabric. If garnet grows with a relatively uniform distribution during prograde metamorphism, the change in position of garnets relative to one another during deformation relates to the type of flow [1].

Case study 3: Morphometric analysis of rodent dentitions to predict dietary niche
Relief and hypsodonty indices were calculated for teeth of fifteen extant rodent species to correlate tooth morphology with dietary niche. Paleoclimates of extinct ecosystems containing fossil rodent teeth may then be predicted by niche-modeling data derived from biogeography of extinct species and diet predicted from dental morphometrics [2]. 3D tooth meshes were constructed, cropped and analyzed in Rapidform using point-cloud surface data generated from microCT scans. Crown curvature, feature extraction, and best-fit planes were used to crop tooth surfaces reproducibly (Fig 3.). $M_2$ mesiodistal length, enamel thickness, orientation patch count rotated (OPCR), and Dirichlet normal energy (DNE) will be the focus of future work.

Case study 4: Bone histology and primary growth rates in hatchling titanosaurs
Two partial skeletons of hatchling *Rapetosaurus krausei,* a titanosaur from the Upper Cretaceous Maevarano Formation of Madagascar [3], were examined to understand early stage growth rates in sauropods. MicroCT was used to garner bone histology data, and preliminary results indicate that primary bone growth in *Rapetosaurus* consists of highly vascularized woven and fibrolamellar bone (Fig. 4). Even in these small juvenile individuals, endosteal remodeling is common at the mid-diaphysis and extends in areas into the mid-cortex. The presence of one line of arrested growth is recorded in each individual [4].

References:
[1] WD Carlson, Mineralogical Magazine **55** (1991), p. 317-330.
[2] JL McGuire, Quaternary International **212** (2010), p. 198-205.
[3] RR Rogers, Geology **33** (2005), p. 297-300.
[4] Funding for the X-ray Computed Tomography lab was provided in part by the University of Minnesota's Infrastructure Investment Initiative. The authors thank the following people for their contributions and allowing us to include their research: Case study 1: Martin Saar, Kong Xiang-Zhao, and Ben Tutulo (UMN GeoFluids); Case study 2: Christian Teyssier, Donna Whitney, and Roxanne Renedo (UMN STAMP); Case study 3: David Fox (UMN Paleontology); Case study 4: Kristina Curry Rogers, Ray Rogers, and Megan Whitney (Macalester College).

**Figure 1.** (left) Reaction vessel setup for in-situ microCT experiments. (right) Dissolution channel developed in dolostone core exposed to flowing brine with dissolved $CO_2$. Yellow dissolution channel illustrates the network of connected pore space mapped using post-experiment microCT scans.

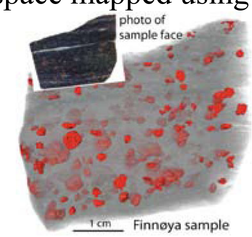


**Figure 2.** 3D rendering of a western gneiss region garnet amphibolite; foliation and metamorphic layering are close to horizontal. Solid red blobs are garnet at the edge of the sample; fainter garnet grains can be seen through the sample.

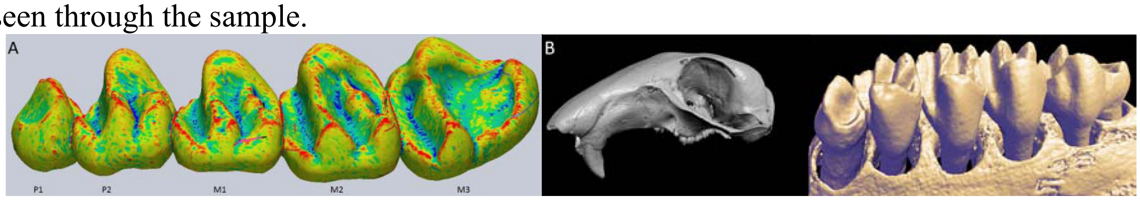


**Figure 3.** (A) *Spermophilus tridecemlineatus* (13-lined ground squirrel) maxillary tooth crowns cropped by curvature map (buccal view). (B) 3D surface of skull reconstruction with close-up of uncropped teeth (lingual view).

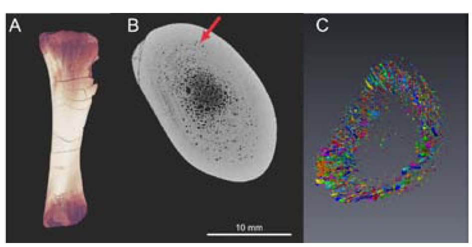


**Figure 4.** (A) Pseudocolored 3D reconstruction of a hatchling *Rapetosaurus* left tibia (12.6 cm long). (B) Mid-diaphyseal cross section of tibia with highly vascularized primary fibrolamellar bone with sparse secondary osteons (red arrow). (C) 3D segmentation of vascularized region from a small portion of the Mid-diaphyseal bone, colors indicate volume of connected regions.